Phase stability of solid solution $La_{1-x}R_xRh_3B$ (R = Gd, Lu and Sc) compounds with cubic anti-perovskite type structure

Kunio Yubuta[a*], Akiko Nomura[b], Kaoru Kouzu[c], Takao Mori[d,e],

Shigeru Okada[c] and Toetsu Shishido[b]

[a] *The Ultramicroscopy Research Center, Kyushu University, Kyushu University, Fukuoka 819-0395, Japan*

[b] *Institute for Materials Research, Tohoku University, Sendai 980-8577, Japan*

[c] *Department of Science and Engineering, Kokushikan University, Tokyo 154-8515, Japan*

[d] *Research Center for Materials Nanoarchitectonics (MANA), National Institute for Materials Science (NIMS), Tsukuba 305-0044, Japan*

[e] *Graduate School of Pure and Applied Science, University of Tsukuba, Tsukuba 305–8671, Japan*

*Corresponding author:
The Ultramicroscopy Research Center, Kyushu University, Fukuoka 819-0395, Japan
Tel: +81-92-802-3488
E-mail: yubuta.kunio.400@m.kyushu-u.ac.jp

Abstract

We have investigated the solid solution range of single phase with a cubic anti-perovskite type structure, and behaviors of lattice parameters, hardness, and thermogravimetry–differential thermal analysis (TG-DTA) in the cubic anti-perovskite type $La_{1-x}R_xRh_3B$ (R = Gd, Lu and Sc) compounds. The cubic anti-perovskite phase exists over the entire composition range x from 0.0 to 1.0 for all La-Gd, La-Lu and La-Sc systems. Both the lattice parameters and the hardness in all La-Gd, La-Lu and

La-Sc systems exhibit a linear dependence on the substitution x for La atom. The results of TG-DTA measurements indicate that the oxidation of the compounds in air starts at about 500-600 K. The mixed phases of RBO$_3$, R_2O$_3$ and Rh are identified as oxidized products around $x = 0.5$. The oxidation onset temperature, and weight gains due to the oxidation depend on substitution x. The behavior of crystallographic and physical/chemical properties in the present compounds $La_{1-x}R_xRh_3B$ strongly depend on the atomic size of the rare-earth atoms forming the cubic framework.

Keywords: cubic anti-perovskite type, solid solution range, X-ray diffraction, TEM, hardness, oxidation resistance.

1. Introduction

Many studies of simple and complex perovskite-type oxides have been investigated because of the interesting features of superconductor, insulator-metallic transition, ion conduction characteristics, dielectric properties, ferroelasticity and so on [1]. Besides, noticeable studies on non-oxide cubic anti-perovskite and Cu_3Au-type compounds [2-4] such as RRh$_3$B$_y$ and RRh$_3$C$_y$, have been performed due to their high phase stability and hardness, which make them promising candidates for some applications at high temperature. R represents rare earth metals and boron (and carbon) site has non-stoichiometry with a range of $0.0 \leq y \leq 1.0$. As shown Fig. 1, R, Rh and B atoms are positioned at

vertices, the face-centered and body-centered sites of the cubic, respectively, in the RRh$_3$B compounds [5]. In addition, theoretical investigations have been carried out by using the first-principle calculations to explain and predict structural, elastic and thermodynamic properties [6-8].

It was reported that the boron content variation in the boron-deficient RRh$_3$B$_y$ compounds induces changes of some properties. Solid solution ranges of boron content for RRh$_3$B$_y$ (R = La, Gd, Lu and Sc) compounds were determined by XRD analysis in Fig. 2(a) [9-13]. As listed in Table I, atomic radii are larger in order of La, Gd, Lu, and Sc. In La-system LaRh$_3$B$_y$, the cubic anti-perovskite phase (space group: $Pm\bar{3}m$) exists only the boron content y equal 1.0. On the other hand, in Sc system ScRh$_3$B$_y$, solid solution range of boron content y extends from 1.0 to 0.0. As indicated by a gray arrow, with increasing atomic size of rare earth atom, solid solution ranges become narrower. Fig. 2(b) shows a relationship between microhardness and lattice parameter for boron full-occupied RRh$_3$B (R = La, Gd, Lu and Sc) compounds [9-13]. As we can easily see, the hardness linearly depends on a size of cubic anti-perovskite lattice. With decreasing the size of lattice (bond length), hardness becomes larger. A similar correlation appears for the boron-deficient RRh$_3$B$_y$ compounds. The correlation between bond length and hardness is consistent with reported results that some properties of RRh$_3$B$_y$ can be tuned by addition of boron located on the center of the rhodium octahedron.

Subsequently, Zeiringer *et al.* carried out the Pd substitution for the Rh sites forming octahedrons [14]. It was investigated regarding the solid solution range for substitution of Rh and Pd atoms, the

behavior of Ce valence and the lattice modulation for $CeRh_{3-z}Pd_zB_{0.5}$ ($0 \leq z \leq 3$) compounds. Although lattice expansion was confirmed, the behavior was not linear with Pd content. Increasing of the lattice size was monotonous at less than $z = 1.5$. The rate of increase was enhanced in the range of $1.5 \leq z \leq 2.4$, and whereas it saturated at larger than $z = 2.4$. Valency and cell volume are intimately related parameters through the Coulomb potential acting on the valence electrons of the atoms. With increasing of Pd content z, the lattice parameter increases, whereas valence of Ce deceases from 4+ to 3+ though the intermediated state.

In the present study, our interest is moved to the framework of cubic lattice formed by rare earth atoms (as indicated by a large arrow in Fig. 1). That is, there was an interest in the possibility of controlling physics and chemical properties by modulation of cubic framework in boron full-occupied $LaRh_3B$ compound by substituting other rare-earth atoms with different size, Gd, Lu and Sc, for La atoms. The scattering power of R atoms is sufficiently large that the structural singularity with the long-range and/or short-range order, if present, can be expected to be detected by X-ray and electron beam. We present results; (i) where the solid solution $La_{1-x}R_xRh_3B$ (R = Gd, Lu and Sc) could be obtained, when rare-earth atoms of different atomic sizes were used together, (ii) the effect of substitution on the hardness and (iii) the changing of the oxidation resistance with substitution.

2. Experimental

Polycrystalline samples of boron full-occupied $La_{1-x}R_xRh_3B$ (R = Gd, Lu and Sc) compounds were synthesized by the arc melting method using 99.9% pure La, Gd, Lu, Sc, Rh and B as raw materials. The button-like product was then turned over and re-melted three times to improve its chemical homogeneity. The synthesized samples were wrapped with Ta foils and annealed at 1573 K for 20 hrs in vacuo. It was confirmed that chemical compositions before and after synthesis are almost the same. In addition, contaminations from an electrode (tungsten) and a hearth (copper) cannot be detected.

Lattice parameters of the polycrystalline samples were determined by powder X-ray diffraction (XRD). The micro-Vickers hardness (H_v) for the samples was measured at room temperature. A load of 300 g was applied for 15 s and 10 impressions were recorded for each sample. The obtained values were averaged. In order to investigate the oxidation resistance, thermo-gravimetric (TG) analysis and differential thermal analysis (DTA) were performed between room temperature and 1473 K to study the oxidation resistance of the samples in air. A sample of about 25 mg was heated at a rate of 10 K/min up to 1473 K. The final oxidation products were analyzed by powder XRD. A grain size of the presented sample is 20–30 μm based on optical microscopy observation. Thin specimens for transmission electron microscopy were prepared by Ar ion milling. Selected area electron diffraction (SAED) patterns taken with the incident beams along three principal directions; [001], [011] and [111], were obtained from same regions using transmission electron microscope (TEM), JEOL JEM-

2000EXII, at accelerating voltage of 200 kV. High-resolution electron micrographs were taken with the incident beams along the [011] direction by using 200 kV TEM, TOPCON EM-002B.

3. Results and Discussion

Powder XRD patterns of boron full-occupied $La_{1-x}Sc_xRh_3B$ compounds are shown in Fig. 3(a). From analysis of powder XRD patterns, it is confirmed that a single phase with cubic anti-perovskite structure (space group: $Pm\bar{3}m$) exists over the entire composition range x from 0.0 to 1.0 for the all systems. It was additionally confirmed that no splitting exhibits at diffraction peaks for all systems. In both La-Gd and La-Lu systems, the cubic anti-perovskite phase also exists without minor phases. Fig. 3(b) summarizes lattice parameters as a function of substitution for three systems. Triangles, squares and circles correspond to the La-Gd, La-Lu and La-Sc systems, respectively. With increasing substitution rare-earth atoms for La atom in all systems, lattice parameters linearly decrease. This tendency is coincident with the result of lattice parameter in Fig. 2(a). On the basis of these results, it can be concluded that the phase relation of cubic anti-perovskite type single-phase linearly depends on the substitution x.

TEM observations were performed in order to clarify the local structure of boron full-occupied $La_{1-x}R_xRh_3B$ compounds. In our previous study, we reported that the observed SAED patterns of $CeRh_3B_{0.5}$ [15,16] and $ScRh_3B_{0.5}$ [17] compounds showed the appearance of 1/2 1/2 1/2–type

superlattice reflections and fine satellite reflections around all Bragg reflections. The 1/2 1/2 1/2–type superstructure was characterized by the structural ordering of both the boron-vacancy and Rh atom in Rh octahedrons. The range of the appearance of 1/2 1/2 1/2-type superlattice reflections and fine satellite ones is consistent with that showing the abrupt drop of hardness, in boron content of $0.4 < x < 0.5$ [10, 18]. In addition, SAED patterns of the Pd substituted $CeRh_{3-z}Pd_zB_{0.5}$ compounds revealed the appearance of 1⁄2 1⁄2 1⁄2–type superstructure and satellite spots with respect to the parent Cu_3Au structure [14]. On the other hand, the 1⁄2 1⁄2 1⁄2–type superstructure is confined to the Rh-rich part of the solid solution $CeRh_{3-z}Pd_zB_{0.5}$, satellite reflections are observed throughout the solid solution.

It was expected that $La_{0.5}Sc_{0.5}Rh_3B$ compound exhibits the most frustrated configuration among the present compounds, because of mixing the largest La and the smallest Sc atoms with a ratio of 1 : 1. Figures 4(a)-(c) show SAED patterns of the $La_{0.5}Sc_{0.5}Rh_3B$ compound, taken with the incident beams along the (a) [001], (b) [011] and (c) [111] directions. Even though there is a large difference of atomic size between La and Sc atoms in the present systems, however one can notice no signs of the structural singularity; *i.e*. superlattice spots, satellite spots and diffuse streaks. Figure 4(d) depicts a high-resolution electron micrograph taken with the incident beam parallel to the [011] direction. The image shows well-ordered and homogeneous bright dots without the displacive and occupancy modulations. These structural features suggest that no lattice modulations exist by the mixing of

$La_{0.5}Sc_{0.5}$. That is, the ordering of the La and Sc atoms does not occur but both La and Sc atoms randomly locate at vertex sites.

It is well known that the hardness is one of representative material parameters indicating the resistance to elastic/plastic deformation. This parameter reflects the nature of the chemical bonding. Figure 5 shows microhardness as a function of substitution x. With increasing substitution rare-earth atoms with small size for La atom, hardness linearly increases. Figure 6 shows a relationship obtained by combined microhardness and lattice parameter. From the result shown in Fig. 6, it can be recognized that there is a strong correlation between hardness and size of lattice (bond length) in boron full-occupied $R$$Rh_3B$ compounds.

In order to elucidate the nature of chemical bonds in the present compounds, TG-DTA measurements were carried out. Figure 7 shows (a) DTA and (b) TG curves of the $La_{1-x}Lu_xRh_3B$ compounds as an example. Size of Lu atom is middle among Gd, Lu and Sc ones. The exothermic peaks at about 500-600 K correspond to oxidation for the present compounds. The oxidation products are listed in Table II. After the exothermic peaks of 500-600 K, LaBO, $LuBO_3$ and Rh_2O_3 were produced around x equal 0.5. On the other hand, the endothermic peaks correspond to the decomposition at about 1300-1400 K. A common feature for all systems is that endothermic peaks appear at same temperature. As a result of thermal reduction, Rh_2O_3 was decomposed and elemental rhodium was obtained above 1300 K, as indicated by endothermic peaks. Oxidation onset temperature,

and weight gains due to the oxidation depend on substitution x as shown Fig. 8. On the other hand, the maximum temperatures of endothermic peaks do not depend on the substitutions.

4. Conclusion

Single-phase of cubic anti-perovskite structure can be obtained over the entire composition range x from 0.0 to 1.0 for $La_{1-x}R_xRh_3B$ (R = Gd, Lu and Sc) compounds based on the powder XRD measurements. Especially, in spite of combination with largest La and smallest Sc atoms, the largest size disparity amongst rare earth elements, the cubic lattice framework of the cubic anti-perovskite structure can be formed without any noticeable modulations. Electron diffraction indicates no structural modulation in the $La_{0.5}Sc_{0.5}Rh_3B$ compound. Both the lattice parameter and the hardness exhibit the linear dependence on the substitution x. By means of TG-DTA, the oxidation of the compounds in air starts at about 500-600 K. Around $x = 0.5$, the mixed phases of RBO_3, R_2O_3 and Rh are identified as oxidized products. On the basis of results, it can be concluded that the behavior of crystallographic and physical/chemical properties in the present compounds strongly depend on the atomic size of the rare-earth atoms forming the cubic framework.

Acknowledgements

KY was partly supported by the Japan Society for the Promotion of Science (JSPS) KAKENHI

(Grants numbers JP19K05643, JP20H05258 and JP23K04373) and the GIMRT program (Proposal numbers 202211-RDKGE-0008, 202212-CRKKE-0020 and 202311-RDKGE-0001) at the Institute for Materials Research, Tohoku University, Japan. TM acknowledges support from JST Mirai Program JPMJMI19A1.

References

[1] M. A. Peña and J. L. G. Fierro, Chem. Rev. **101** (2001) 1981–2018.

[2] H. Holleck, J. Less-Common Met. **52** (1977) 167–712.

[3] P. Rogl, L. Delong, J. Less-Common Met. **91** (1983) 97–106.

[4] S. K. Malik, S. K. Dhar, R. Vijayaraghavan, Bull. Mater. Sci. **6** (1984) 263–272.

[5] H. Takei and T. Shishido, J. Less-Common Met. **97** (1984) 223–229.

[6] R. Sahara, T. Shishido, A. Nomura, K. Kudou, S. Okada, V. Kumar, K. Nakajima, Y. Kawazoe, Comp. Mater. Sci. **36** (2006) 12–16.

[7] F. Litimein, R. Khenata, A. Bouhemadou, Y. Al-Douri, S. Bin Omran, Molecular Phys. **110** (2012) 121–128.

[8] A. Bouhemadou, G. Uğur, Ş. Uğur, F. Soyalp, R. Khenata, S. Bin-Omran, Comp. Mater. Sci. **54** (2012) 336–344.

[9] T. Shishido, H. Yamauchi, K. Kudou, S. Okada, J. Ye, A. Yoshikawa, H. Horiuchi, T. Fukuda, Jpn. J. Appl. Phys. **36** (1997) L1436.

[10] T. Shishido, J. Ye, S. Okada, K. Kudou, T. Sasaki, S. Isida, T. Naka, M. Oku, I. Higashi, H. Kishi, H. Horiuchi, T. Fukuda, J. Alloys Compd. **309** (2000) 107–112.

[11] T. Shishido, J. Ye, K. Kudou, S. Okada, M. Oku, H. Horiuchi, T. Fukuda, J. Ceram. Soc. Jpn. **108** (2000) 683–686.

[12] T. Shishido, K. Kudou, S. Okada, J. Ye, A. Yoshikawa, T. Sasaki, M. Oku, H. Horiuchi, I. Higashi, S. Kohiki, Y. Kawazoe, K. Nakajima, Jpn. J. Appl. Phys. **40** (2001) 6037–6038.

[13] T. Shishido, J. Ye, S. Okada, K. Kudou, K. Iizumi, M. Oku, Y. Ishizawa, R. Sahara, V. Kumar, A. Yoshikawa, M. Tanaka, H. Horiuchi, A. Nomura, T. Sugawara, K. Obara, T. Amano, S. Kohiki, Y. Kawazoe, K. Nakajima, J. Alloys Compd. **408-412** (2006) 379–383.

[14] I. Zeiringer, J.G. Sereni, M.G. Berisso, K. Yubuta, P. Rogl, A. Grytsiv, E. Bauer, Mater. Res.

Express **1** (2014) 016101.

[15] K. Yubuta, A. Nomura, K. Nakajima, T. Shishido, J. Alloys Compd. **426** (2006) 308–311.

[16] K. Yubuta, A. Nomura, T. Yamamura, T. Shishido, J. Alloys Compd. **451** (2008) 301–304.

[17] K. Yubuta, A. Nomura, K. Nakajima, T. Shishido, J. Alloys Compd. **471** (2009) 341–346.

[18] T. Shishido, M. Oku, S. Okada, K. Kudou, K. Iizumi, S. Sawada, Y. Yoshizawa, A. Nomura, T. Sugawara, K. Obara, R. Sahara, K. Yubuta, H. Kojima, V. Kumar, M. Tanaka, K. Shimamura, S. Oishi, S. Koshiki, Y. Kawazoe, K. Nakajima, J. Alloys Compd. **426** (2006) 304–307.

Table I. Atomic size of rare-earth atoms

R	atomic size of *R*/ nm
La	0.188
Gd	0.180
Lu	0.173
Sc	0.161

Table II. Oxidation products heated up to 1473 K in air after the oxidation process for $La_{1-x}Lu_xRh_3B$ compounds

x	oxidation products
0.0	$LaBO_3$ + Rh
0.2	$LaBO_3$ + Lu_2O_3 + Rh
0.4	$LaBO_3$ + $LuBO_3$ + Rh
0.6	$LaBO_3$ + $LuBO_3$ + Rh
0.8	$LuBO_3$ + Rh
1.0	$LuBO_3$ + Rh

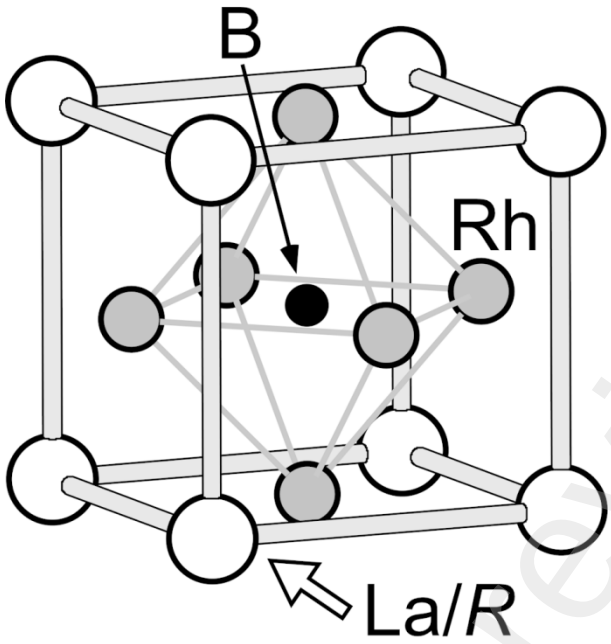

Fig. 1 Crystal structure of cubic anti-perovskite type $R\mathrm{Rh_3B}$.

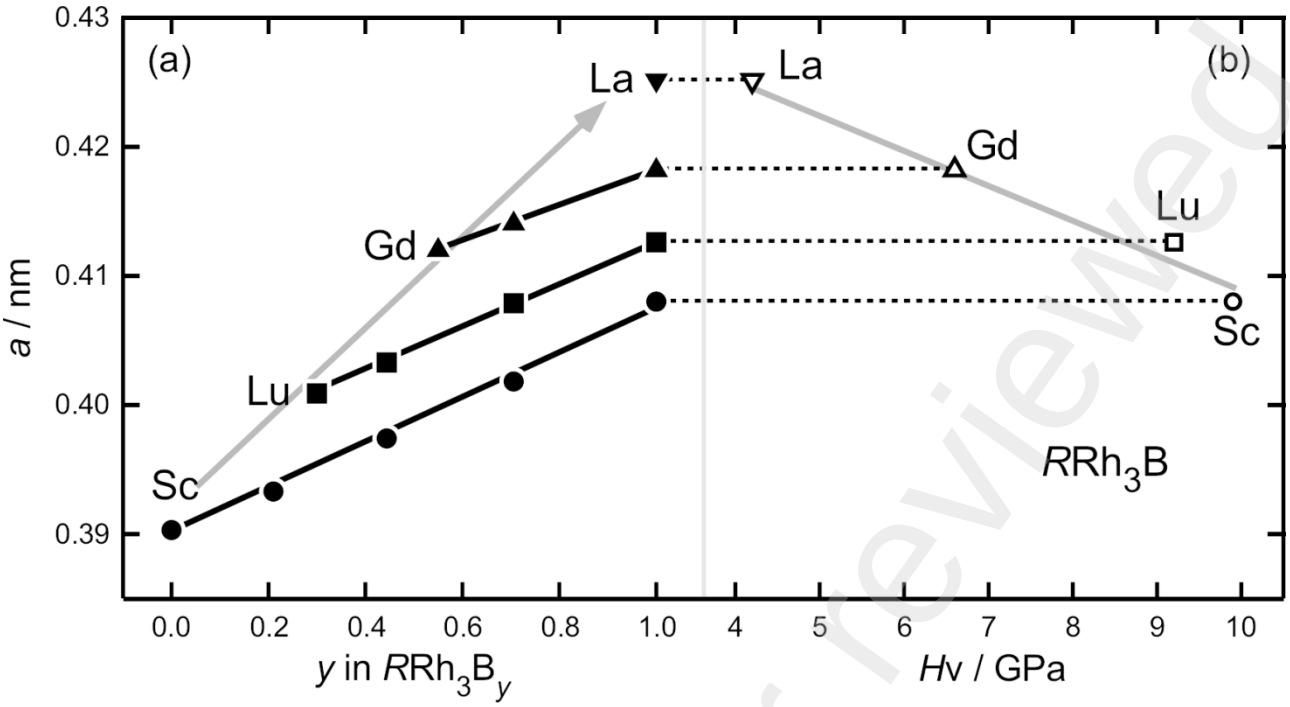

Fig. 2 (a) Solid solution ranges of boron content with lattice parameters for boron-deficient RRh$_3$B$_y$ (R = La, Gd, Lu and Sc) compounds. (b) Relationship between microhardness and lattice parameter for boron full-occupied RRh$_3$B (R = La, Gd, Lu and Sc) compounds.

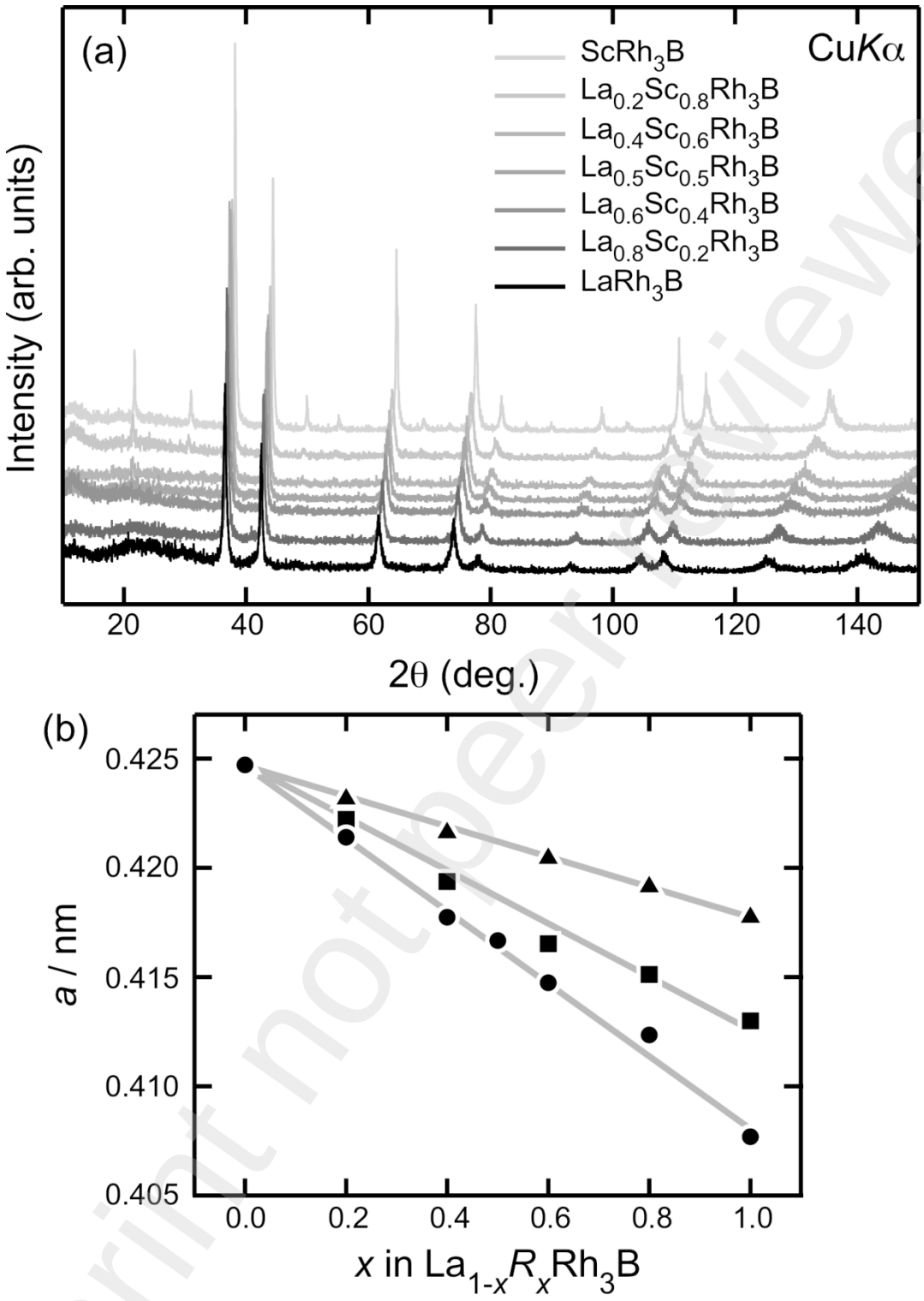

Fig. 3 (a) XRD patterns of $La_{1-x}Sc_xRh_3B$ compounds. (b) Lattice parameters as a function of substitution for three systems. Triangles, squares and circles correspond to the La-Gd, La-Lu and La-Sc systems, respectively.

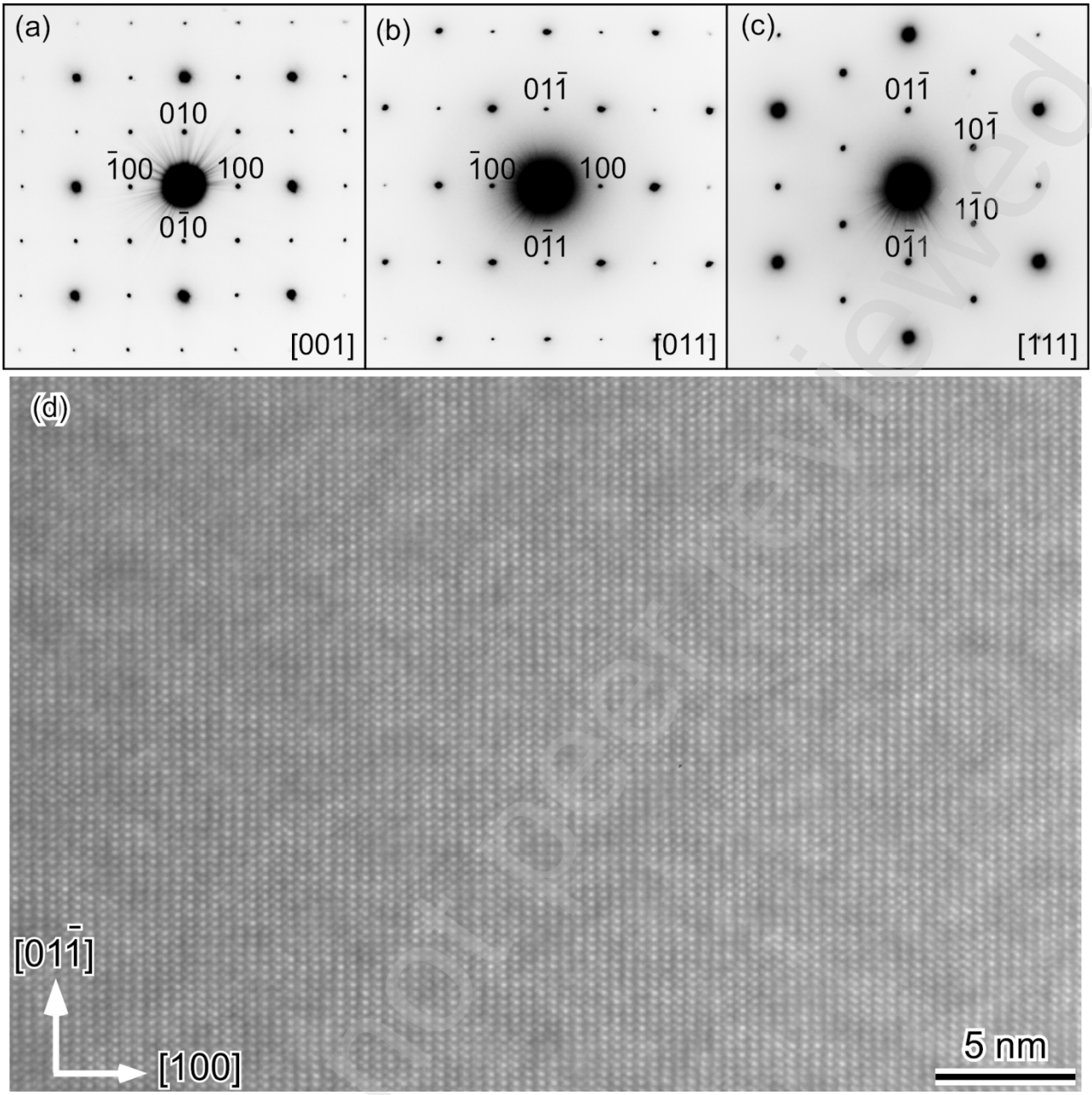

Fig. 4 Electron diffraction patterns of the $La_{0.5}Sc_{0.5}Rh_3B$ compound, taken with incident beams parallel to (a) [001], (b) [011] and (c) [111] directions. Reflections are indexed with the cubic anti-perovskite type structure. (d) High-resolution electron micrograph taken with the incident beam parallel to the [011] direction.

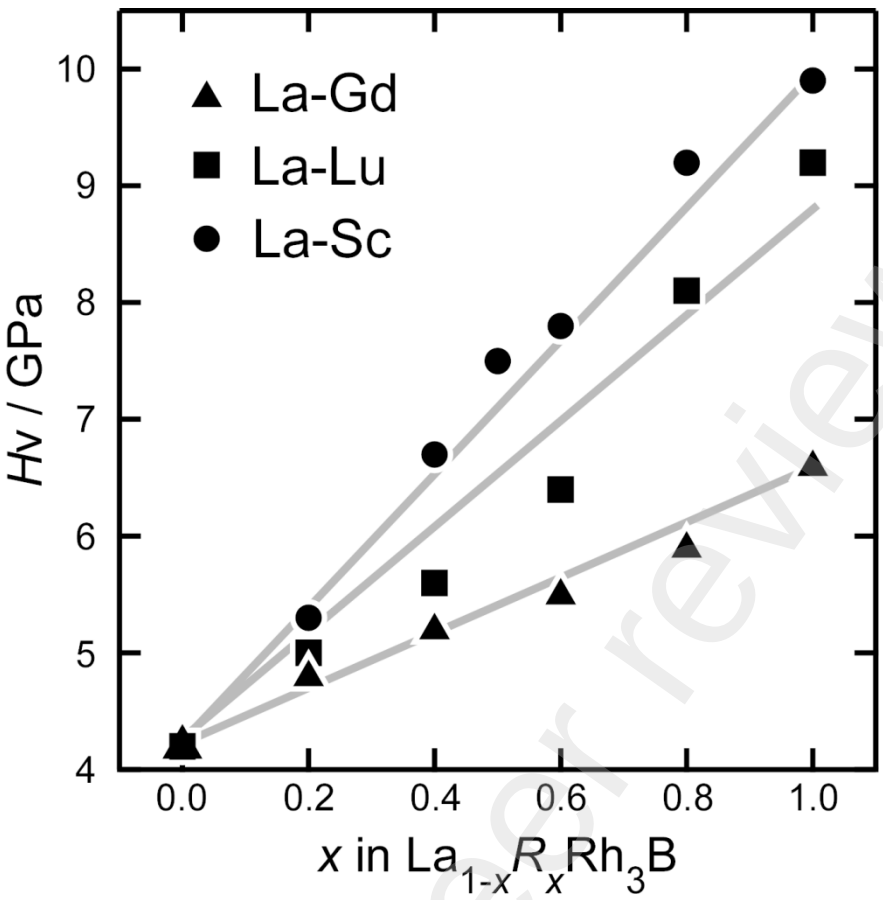

Fig. 5 Microhardness as a function of substitution *x*. Triangles, squares and circles correspond to the La-Gd, La-Lu and La-Sc systems, respectively.

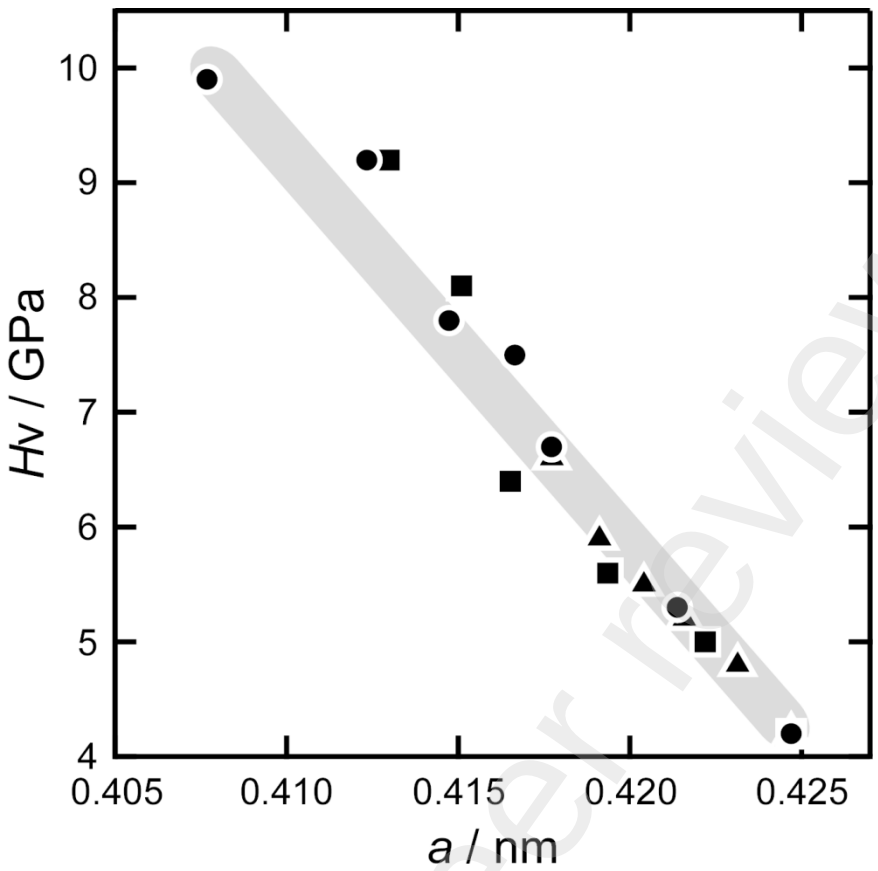

Fig. 6 Relationship between microhardness and lattice parameter. Triangles, squares and circles correspond to the La-Gd, La-Lu and La-Sc systems, respectively.

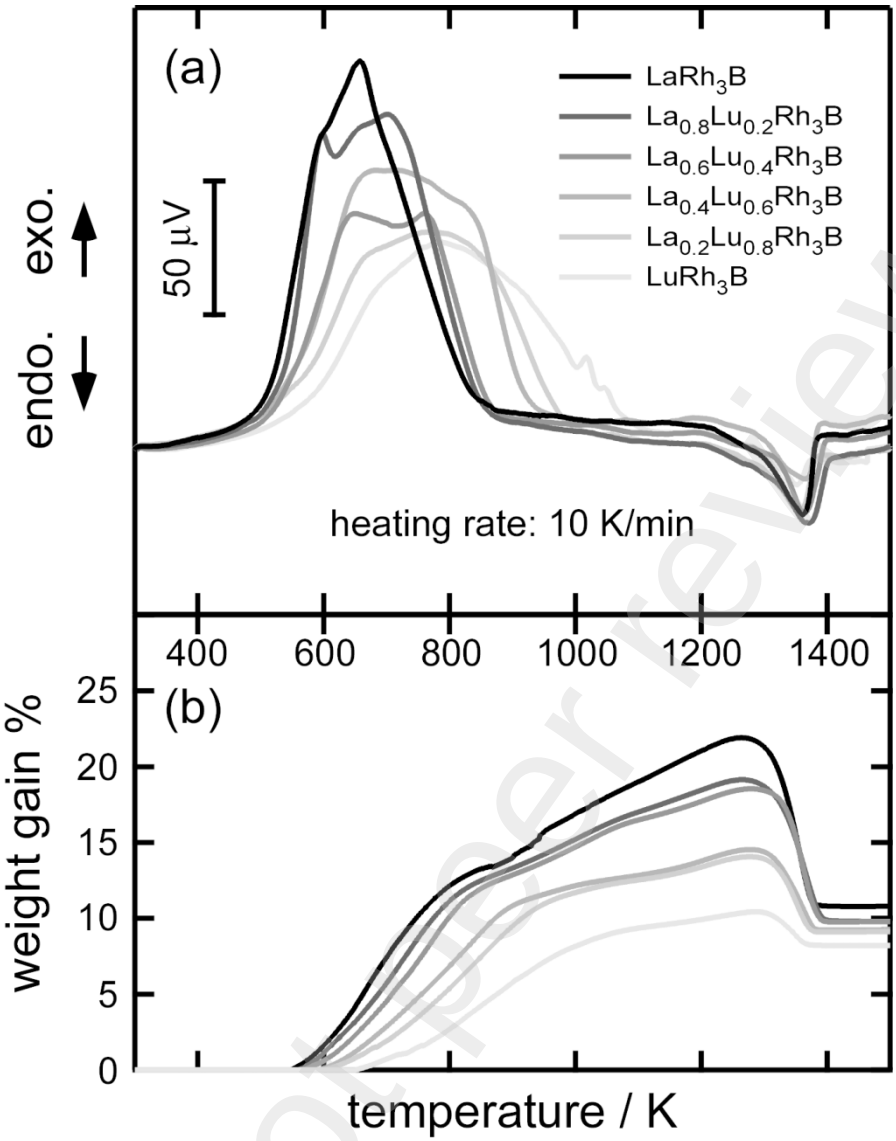

Fig. 7 (a) DTA and (b) TG curves of the $La_{1-x}Lu_xRh_3B$ compounds.

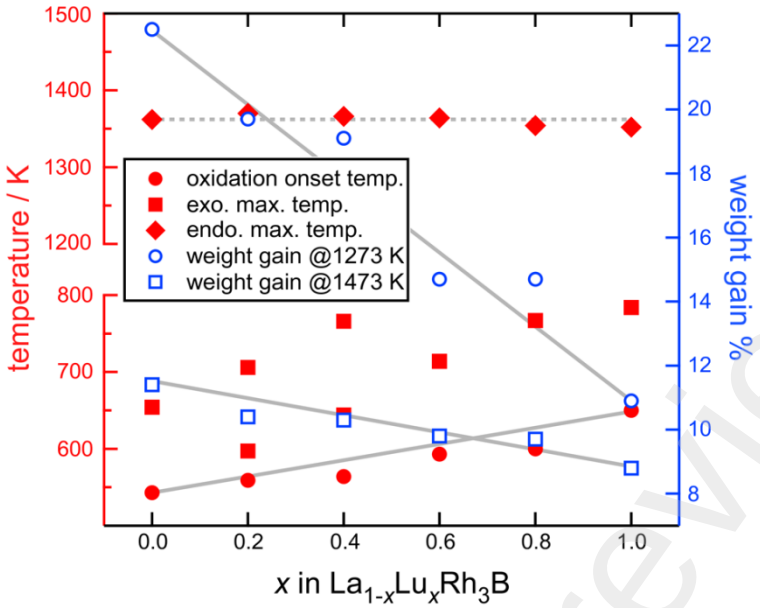

Fig. 8 Oxidation onset temperature and weight gains as a function of substitution x for the $La_{1-x}Lu_xRh_3B$ compounds.

Graphical abstract

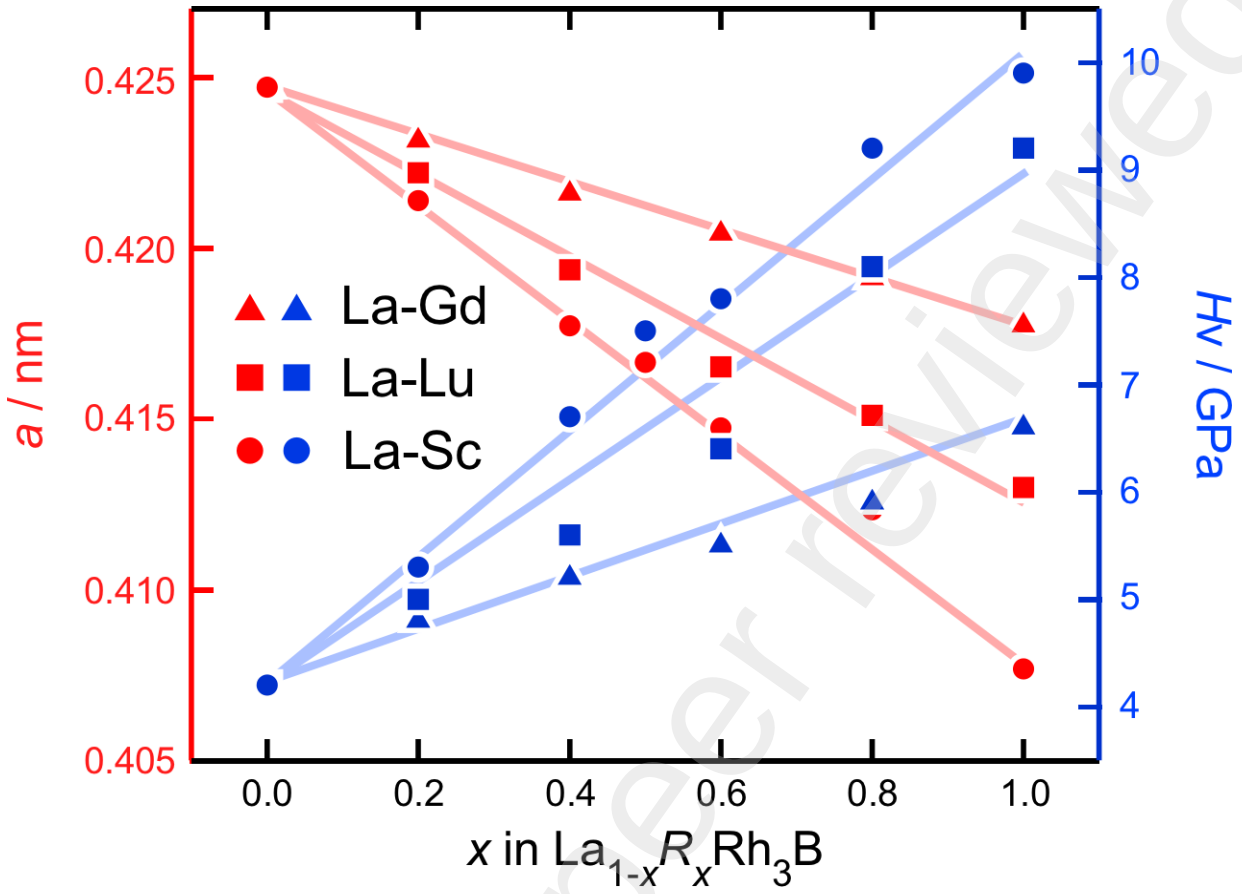

Highlights

► The cubic anti-perovskite phase exists over the entire composition range x from 0.0 to 1.0 for $La_{1-x}R_xRh_3B$ (R = Gd, Lu and Sc) compounds. Both lattice parameter and the hardness exhibit a linear dependence on the substitution x.

► TG-DTA measurements indicate that the oxidation of the compounds in air starts at about 500-600 K. A mixed phase of RBO_3, R_2O_3 and Rh is identified as oxidized products around x = 0.5.